

# SCIENTIFIC REPORTS

OPEN

## Relation between the Co-O bond lengths and the spin state of Co in layered Cobaltates: a high-pressure study

Yi-Ying Chin<sup>1</sup>, Hong-Ji Lin<sup>1</sup>, Zhiwei Hu<sup>2</sup>, Chang-Yang Kuo<sup>2</sup>, Daria Mikhailova<sup>2,3,4</sup>, Jenn-Min Lee<sup>1</sup>, Shu-Chih Haw<sup>1</sup>, Shin-An Chen<sup>1</sup>, Walter Schnelle<sup>2</sup>, Hirofumi Ishii<sup>1</sup>, Nozomu Hiraoka<sup>1</sup>, Yen-Fa Liao<sup>1</sup>, Ku-Ding Tseui<sup>1</sup>, Arata Tanaka<sup>5</sup>, Liu Hao Tjeng<sup>2</sup>, Chien-Te Chen<sup>1</sup> & Jin-Ming Chen<sup>1</sup>

The pressure-response of the Co-O bond lengths and the spin state of Co ions in a hybrid 3d-5d solid-state oxide  $\text{Sr}_2\text{Co}_{0.5}\text{Ir}_{0.5}\text{O}_4$  with a layered  $\text{K}_2\text{NiF}_4$ -type structure was studied by using hard X-ray absorption and emission spectroscopies. The Co- $K$  and the Ir- $L_3$  X-ray absorption spectra demonstrate that the Ir<sup>5+</sup> and the Co<sup>3+</sup> valence states at ambient conditions are not affected by pressure. The Co  $K\beta$  emission spectra, on the other hand, revealed a gradual spin state transition of Co<sup>3+</sup> ions from a high-spin ( $S = 2$ ) state at ambient pressure to a complete low-spin state ( $S = 0$ ) at 40 GPa without crossing the intermediate spin state ( $S = 1$ ). This can be well understood from our calculated phase diagram in which we consider the energies of the low spin, intermediate spin and high spin states of Co<sup>3+</sup> ions as a function of the anisotropic distortion of the octahedral local coordination in the layered oxide. We infer that a short in-plane Co-O bond length ( $< 1.90 \text{ \AA}$ ) as well as a very large ratio of  $\text{Co-O}_{\text{apex}}/\text{Co-O}_{\text{in-plane}}$  is needed to stabilize the IS Co<sup>3+</sup>, a situation which is rarely met in reality.

Layered perovskites  $\text{A}_2\text{BO}_4$  with a  $\text{K}_2\text{NiF}_4$ -type structure have been intensively investigated owing to their unique properties, such as high-temperature superconductivity in cuprates, spin-triplet superconductivity in ruthenates, spin/charge stripes in nickelates and manganites<sup>1</sup>. Recently,  $\text{Sr}_2\text{IrO}_4$  with low-spin (LS) Ir<sup>4+</sup> has attracted much attention because of the insulating behavior resulting from the strong spin-orbit interaction<sup>2,3</sup>, while  $\text{Sr}_2\text{CoO}_4$  exhibits a metallic behavior because of its intermediate-spin (IS) Co<sup>3+</sup> coming from both the negative charge-transfer energy and the tetragonal distortion<sup>4-10</sup>. In  $\text{La}_{2-x}\text{Sr}_x\text{CoO}_4$ , the  $\text{CoO}_6$  octahedron has an elongated distortion, and thus the IS Co<sup>3+</sup> state might be stabilized owing to the single occupation in the  $e_g$  levels. Therefore, the spin state of the Co<sup>3+</sup> ions in  $\text{La}_{2-x}\text{Sr}_x\text{CoO}_4$  has been controversially discussed as a pure IS state or alternatively as a mixture of high spin (HS) Co<sup>3+</sup> and low-spin (LS) Co<sup>3+</sup><sup>11-16</sup>. There are also conflicting results in the pressure-driven spin crossover of Co<sup>3+</sup> ion in the layered compound  $\text{Sr}_2\text{CoO}_3\text{F}$  with the  $\text{K}_2\text{NiF}_4$ -type structure<sup>17</sup>. First principle calculations predicted the HS state at ambient pressure and the IS state under high pressure<sup>18</sup>, while Co  $K\beta$  emission experiments suggested a complete HS-LS transition at 12 GPa without through an IS state<sup>19</sup>. Therefore, the presence of the IS Co<sup>3+</sup> is still under fierce debate.

The hybrid Co/Ir solid-state oxide  $\text{Sr}_2\text{Ir}_{2-x}\text{Co}_x\text{O}_4$  system might show unusual electronic and magnetic structures considering the presence of strong intra-atomic multiplet interactions for the localized Co 3d electrons and a large spin-orbit coupling for the delocalized Ir 5d electrons. As indicated by a previous study, the substitution of Ti, Fe, and Co for Ir in  $\text{Sr}_2\text{IrO}_4$  induces a reduction of the magnetic susceptibility as well as an enhancement of the effective paramagnetic moment for samples with Co and Fe together with a suppression of the weak ferromagnetic ordering<sup>20</sup>. On the other hand, substituting Mn for Ir results in the reordering and flipping of the spins

<sup>1</sup>National Synchrotron Radiation Research Center, Hsinchu, 30076, Taiwan. <sup>2</sup>Max Planck Institute for Chemical Physics of Solids, Dresden, D-01187, Germany. <sup>3</sup>Karlsruhe Institute of Technology (KIT), Institute for Applied Materials (IAM), Eggenstein-Leopoldshafen, D-76344, Germany. <sup>4</sup>Institute for Complex Materials, IFW Dresden, Dresden, D-01069, Germany. <sup>5</sup>Department of Quantum Matter, ADSM, Hiroshima University, Higashi-Hiroshima, 739-8530, Japan. Correspondence and requests for materials should be addressed to H.-J.L. (email: [hjlin@nsrrc.org.tw](mailto:hjlin@nsrrc.org.tw)) or J.-M.C. (email: [jmchen@nsrrc.org.tw](mailto:jmchen@nsrrc.org.tw))

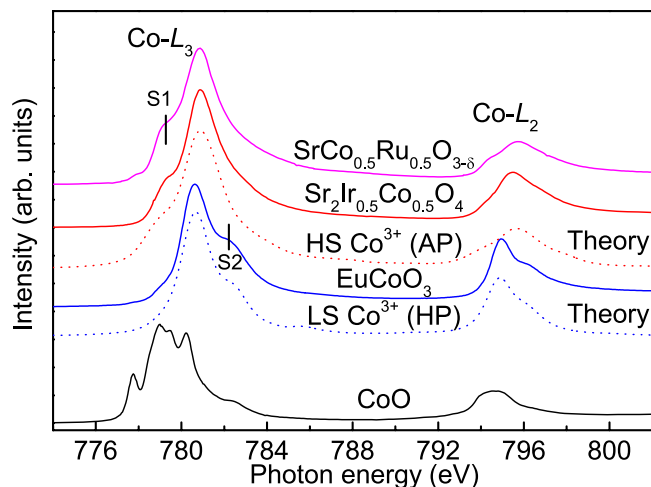


**Figure 1.** Co- $L_{2,3}$  absorption spectra of  $\text{Sr}_2\text{Co}_{0.5}\text{Ir}_{0.5}\text{O}_4$  together with  $\text{EuCoO}_3$  as a LS- $\text{Co}^{3+}$  ref. 24,  $\text{SrCo}_{0.5}\text{Ru}_{0.5}\text{O}_{3-\delta}$  as a HS- $\text{Co}^{3+}$  ref. 29, and  $\text{CoO}$  as a HS- $\text{Co}^{2+}$  reference. The theoretical spectra of HS  $\text{Co}^{3+}$  below  $\text{Sr}_2\text{Co}_{0.5}\text{Ir}_{0.5}\text{O}_4$  and LS  $\text{Co}^{3+}$  below  $\text{EuCoO}_3$  are also included for comparison.

as well as a decrease of the magnetic ordering temperature<sup>21</sup>. Co in  $\text{Sr}_2\text{Ir}_{1-x}\text{Co}_x\text{O}_4$  is proposed to be in 4+ valence state for Co concentrations up to 30%, while the effective magnetic moment ( $4.69 \mu_B$ ) falls in between what is expected for IS  $\text{Co}^{4+}$  ( $3.87 \mu_B$ ) and high spin (HS)  $\text{Co}^{4+}$  ( $5.92 \mu_B$ )<sup>20</sup>. However, a later theoretical study proposed the presence of a charge-spin-orbital state in Fe- or Co-doped  $\text{Sr}_2\text{IrO}_4$  with HS  $\text{Fe}^{3+}$  and HS  $\text{Co}^{3+}$  instead of IS  $\text{Fe}^{4+}$  and IS  $\text{Co}^{4+}$ <sup>22</sup>. The spin state degree of freedom of Co results from subtle balance between crystal field splitting and Hund's rule exchange energy. Pure Low-spin (LS)  $\text{Co}^{3+}$  is well known, such as  $\text{LiCoO}_2$ ,  $\text{NaCoO}_2$ , and  $\text{EuCoO}_3$ , while pure high-spin (HS)  $\text{Co}^{3+}$  exists only in systems with the relatively weak crystal field like  $\text{YBa}_2\text{Co}_4\text{O}_7$  with  $\text{CoO}_4$  tetrahedrons<sup>23</sup> and  $\text{Sr}_2\text{CoO}_3\text{Cl}$  with  $\text{CoO}_5$  pyramids<sup>24</sup>. The HS  $\text{Co}^{3+}$  with  $\text{CoO}_6$  symmetry in cobalt oxides was only found in the system with a mixture of HS and LS like  $\text{LaCoO}_3$ <sup>25</sup> or in the system with oxygen deficiency such as  $\text{GdBaCo}_2\text{O}_{5.5}$ <sup>26</sup>. Considering that  $\text{Sr}_2\text{IrO}_4$  has relatively large lattice parameters ( $\text{Ir-O}_{\text{in-plane}} = 1.9832 \text{ \AA}$ )<sup>27</sup>, it is expected that the  $\text{Co}^{3+}$  ions doped in  $\text{Sr}_2\text{IrO}_4$  would be in a pure HS state owing to the weak crystal field. However, pressure dependence of crystal-structure study on  $\text{Sr}_2\text{Co}_{0.5}\text{Ir}_{0.5}\text{O}_4$  has shown a sharp increase of the  $c/a$  ratio with pressures up to 10 GPa<sup>28</sup>. This increase in the tetragonal distortion should favor the IS  $\text{Co}^{3+}$  state. Furthermore,  $\text{Sr}_2\text{Co}_{0.5}\text{Ir}_{0.5}\text{O}_4$  exhibits a negative Weiss constant, indicating a dominant antiferromagnetic interaction in this system<sup>28</sup>, which might be related to the spin state of Co. In this work, we have investigated the relation between the Co-O bond lengths and the spin states of  $\text{Co}^{3+}$  ions in  $\text{Sr}_2\text{Co}_{0.5}\text{Ir}_{0.5}\text{O}_4$  under external pressures. We have drawn a phase diagram of the spin state of a  $\text{Co}^{3+}$  ion as a function of the anisotropic Co-O bond lengths.

## Results

**Co- $L_{2,3}$  X-ray absorption.** The Co- $L_{2,3}$  XAS spectrum of  $\text{Sr}_2\text{Co}_{0.5}\text{Ir}_{0.5}\text{O}_4$  is presented in Fig. 1 together with those of  $\text{EuCoO}_3$  as a LS- $\text{Co}^{3+}$  reference,  $\text{SrCo}_{0.5}\text{Ru}_{0.5}\text{O}_{3-\delta}$  as a HS- $\text{Co}^{3+}$  reference, and  $\text{CoO}$  as a high-spin (HS)  $\text{Co}^{2+}$ <sup>24,29</sup>. One can see that the center of gravity of the  $L_3$  white line of  $\text{Sr}_2\text{Co}_{0.5}\text{Ir}_{0.5}\text{O}_4$  (red line) is at a higher photon energy as compared to that of  $\text{CoO}$ , while it is similar to that of  $\text{EuCoO}_3$  and  $\text{SrCo}_{0.5}\text{Ru}_{0.5}\text{O}_{3-\delta}$ . This establishes that the Co in  $\text{Sr}_2\text{Co}_{0.5}\text{Ir}_{0.5}\text{O}_4$  is trivalent, different from the parent compound  $\text{Sr}_2\text{CoO}_4$  with  $\text{Co}^{4+}$ . Moreover, the line shape of the  $\text{Sr}_2\text{Co}_{0.5}\text{Ir}_{0.5}\text{O}_4$  spectrum is very different from that of  $\text{EuCoO}_3$ , implying a different local electronic structure. As shown in previous studies, the presence of the low-energy shoulder S1 at the  $\text{Co}^{3+}$   $L_3$  edge is characteristic for the high-spin state, while the high-energy shoulder S2 is indicative for the low-spin state<sup>24,29</sup>. The similarity between  $\text{Sr}_2\text{Co}_{0.5}\text{Ir}_{0.5}\text{O}_4$  and  $\text{SrCo}_{0.5}\text{Ru}_{0.5}\text{O}_{3-\delta}$  also shows the same spin state, namely HS. To further confirm HS  $\text{Co}^{3+}$  in  $\text{Sr}_2\text{Co}_{0.5}\text{Ir}_{0.5}\text{O}_4$ , we performed the configuration-interaction cluster calculations including the full atomic multiplet, and the crystal field interactions, as well as the hybridization between the Co and oxygen ions according to Harrison's prescription<sup>30,31</sup>. The parameter values are listed in ref. 32. The theoretical HS  $\text{Co}^{3+}$  spectrum was plotted below  $\text{Sr}_2\text{Co}_{0.5}\text{Ir}_{0.5}\text{O}_4$ . One can observe that the HS- $\text{Co}^{3+}$  scenario nicely reproduces all features of the experimental spectrum, further demonstrating the HS  $\text{Co}^{3+}$  ground state in this system. We would like to note that the 3+ valence of the Co is fully consistent with the finding of the 5+ valence of the Ir ion as demonstrated in the previous study by the Ir- $L_3$  XAS spectrum<sup>28</sup>.

**Co-K X-ray absorption under pressure.** We now investigate the Co spin state as a function of pressure using hard X-rays. The spin state can be determined also by the Co-K XAS spectra, since different spin states possess distinct electronic structures. The Co-K XAS spectra at ambient pressure and at 43 GPa are shown in Fig. 2. The XAS spectra contain two broad features in the pre-edge region around 7710 eV, and one intense absorption peak around 7725 eV. The main peak can be attributed to the dipole transition from the Co 1s core level to the Co 4p unoccupied states, while the pre-edge structures can be assigned to transitions from the Co 1s to the Co 3d  $t_{2g}$  and  $e_g$  levels owing to the hybridization between Co 3d and 4p states<sup>33</sup>. As shown in the inset of Fig. 2, one observes a spectral weight transfer with pressure: the low-energy feature P1 loses its spectral intensity, while

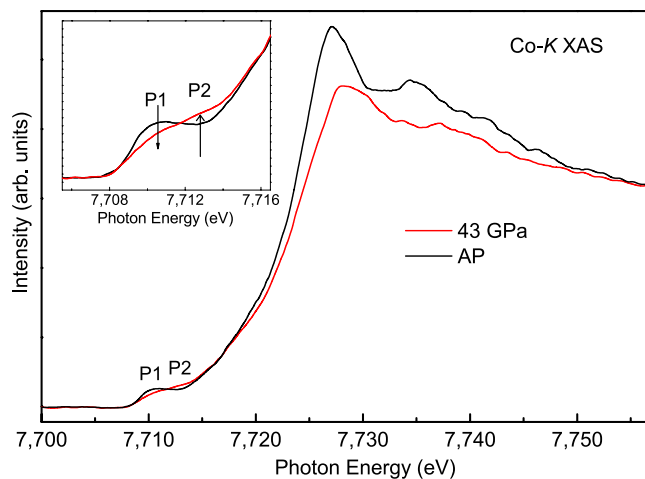


**Figure 2.** The Co-K PFY XAS spectra of  $\text{Sr}_2\text{Co}_{0.5}\text{Ir}_{0.5}\text{O}_4$  at ambient pressure and 43 GPa.

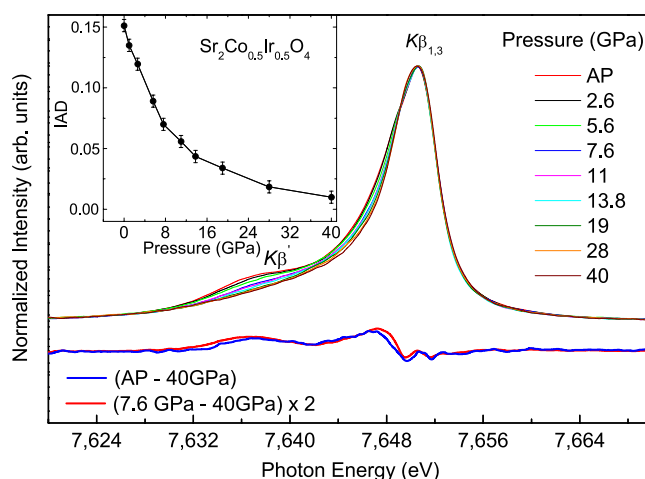


**Figure 3.** Co  $K\beta$  X-ray emission spectra (XES) of  $\text{Sr}_2\text{Co}_{0.5}\text{Ir}_{0.5}\text{O}_4$  and difference spectra of Co  $K\beta$  emissions between ambient pressure (AP) and 40 GPa (blue line) and between 7.6 and 40 GPa (red line). Inset: Integrated absolute difference (IAD) as a function of pressure for  $\text{Sr}_2\text{Co}_{0.5}\text{Ir}_{0.5}\text{O}_4$ .

the feature P2 gains its spectral intensity. As indicated by the charge-transfer multiplet calculation in an earlier study<sup>34</sup>, the LS state has only one single peak in the pre-edge range, while both the IS and HS states possess two features because of the accessible  $t_{2g}$  levels in the higher spin states. Since the IS and HS states only have relatively small line shape differences, the strong spectral change implies the increase of the LS content with pressure<sup>34</sup>. Moreover, the raising edge is also shifted to higher photon energies with pressure. This shift is consistent with the spin state transition from the HS  $\text{Co}^{3+}$  to LS  $\text{Co}^{3+}$ , since the latter has a larger band gap. All this is consistent with the findings of the temperature-dependence Co-K XAS studies on  $\text{LaCoO}_3$  and  $(\text{Pr}_{0.7}\text{Sm}_{0.3})_{0.7}\text{Ca}_{0.3}\text{CoO}_3$ <sup>34,35</sup>, in which the Co-K absorption edge of the low spin  $\text{Co}^{3+}$  at the low temperature is at higher photon energies compared to that of the higher spin  $\text{Co}^{3+}$ .

**Co-KX-ray emission under pressure.** To identify the pressure-induced spin state transition of HS- $\text{Co}^{3+}$ , we have collected the Co- $K\beta$  emission spectra of  $\text{Sr}_2\text{Co}_{0.5}\text{Ir}_{0.5}\text{O}_4$  in the pressure range between ambient pressure and 40 GPa as shown in Fig. 3. The ambient-pressure Co  $K\beta$  emission spectrum represents a main peak located at  $\sim 7,650$  eV corresponding to the  $K\beta_{1,3}$  line, and a pronounced satellite peak at  $\sim 7,637$  eV corresponding to the  $K\beta'$  line. This line shape is typical for the HS- $\text{Co}^{3+}$  state, as obtained in the compounds with HS- $\text{Co}^{3+}$  like  $\text{SrCo}_{0.5}\text{Ru}_{0.5}\text{O}_{3-\delta}$ <sup>29</sup> or  $\text{LaCoO}_3$  at high temperature<sup>34</sup>. The intensity ratio of the low-energy  $K\beta'$  line to the main emission  $K\beta_{1,3}$  line is proportional to the number of the unpaired electrons in the incomplete 3d shell<sup>36</sup> and can be used for an indication of spin states in the material<sup>29,33-35</sup>. With increasing pressure, the intensity of the low-energy  $K\beta'$  line decreases and almost disappears at 40 GPa (Fig. 3). Figure 4 presents the Co  $K\beta$  XES data of  $\text{Sr}_2\text{Co}_{0.5}\text{Ir}_{0.5}\text{O}_4$  at AP and 40 GPa together with those of  $\text{Sr}_2\text{CoO}_3\text{F}$  at 1 GPa (HS) and 17 GPa (LS) as well as those of  $\text{LaCoO}_3$  at 17 K (LS) and 803 K (mainly HS)<sup>19,34</sup>. To compare the intensity ratio of the  $K\beta_{1,3}$  line and the  $K\beta'$  line, those data are aligned and normalized to the  $K\beta_{1,3}$  peak. As shown in Fig. 4, the reduction of the  $K\beta'$  spectral weight in  $\text{Sr}_2\text{Co}_{0.5}\text{Ir}_{0.5}\text{O}_4$  is the same as that of  $\text{Sr}_2\text{CoO}_3\text{F}$ <sup>19</sup> indicating the complete HS-LS state transition in

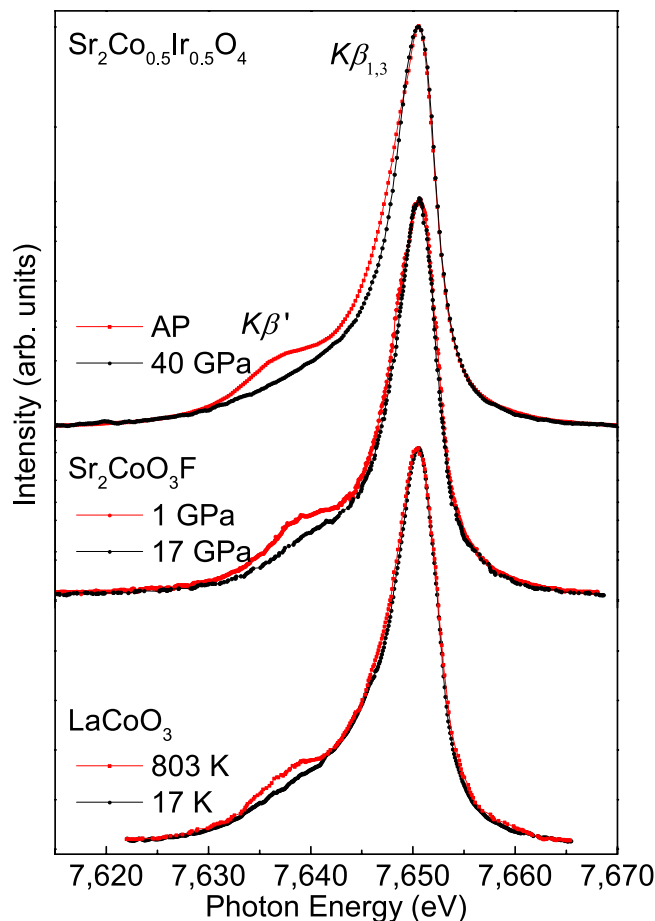


**Figure 4.** Co  $K\beta$  X-ray emission spectra (XES) of  $\text{Sr}_2\text{Co}_{0.5}\text{Ir}_{0.5}\text{O}_4$  at ambient pressure (red line) and 40 GPa (blue line) together with those of  $\text{Sr}_2\text{CoO}_3\text{F}$ <sup>19</sup> at 1 GPa (HS) and 17 GPa (LS) and those of  $\text{LaCoO}_3$ <sup>34</sup> at 17 K (LS) and 803 K (mainly HS).

$\text{Sr}_2\text{Co}_{0.5}\text{Ir}_{0.5}\text{O}_4$  up to 40 GPa. But the decrease of the  $K\beta'$  spectral weight is much larger than that of  $\text{LaCoO}_3$ <sup>34</sup> from 803 K to 17 K, since the spin state transition in the latter is not complete in this temperature range. Furthermore, the inset of Fig. 3 presents integrated absolute difference (IAD) as a function of pressure<sup>33–35</sup>, and the total IAD changes by about 0.14 from ambient pressure to 40 GPa. This value is similar to that of  $\text{SrCo}_{0.5}\text{Ru}_{0.5}\text{O}_{3-\delta}$ <sup>29</sup> and consistent with what is expected for a complete HS ( $S=2$ ) to LS ( $S=0$ ) transition<sup>37</sup>.

At 7.6 GPa, the IAD value of  $\sim 0.07$  corresponds to the change in the spin state  $\Delta S=1$ , comparing with the value at ambient pressure. Two possible scenarios may satisfy the averaged spin state with  $S=1$ : either the existence of intermediate spin state of  $\text{Co}^{3+}$  (IS- $\text{Co}^{3+}$ ,  $S=1$ ) or a coexistence of equal amounts of HS- $\text{Co}^{3+}$  ( $S=2$ ) and LS- $\text{Co}^{3+}$  ( $S=0$ ). The presence of IS- $\text{Co}^{3+}$  in perovskite-like oxides is a matter of long-time discussions, especially for  $\text{LaCoO}_3$ <sup>34,38,39</sup> and other rare-earth metal cobaltates<sup>40</sup>. In the case of layered perovskites, the reported results about spin-state crossover of the  $\text{Co}^{3+}$  ions are also controversial: for example, upon replacement of  $\text{La}^{3+}$  by the larger  $\text{Sr}^{2+}$  in  $\text{La}_{2-x}\text{Sr}_x\text{CoO}_4$  a drastic change of magnetic and electronic properties was ascribed to a spin-state transition of  $\text{Co}^{3+}$  from a high-spin to an intermediate-spin<sup>41</sup>. On the other hand, spin state transition from the LS- $\text{Co}^{3+}$  to HS- $\text{Co}^{3+}$  upon the increase of temperature was reported for single crystals of  $\text{La}_{2-x}\text{Sr}_x\text{CoO}_4$ , based also on susceptibility data analysis<sup>14</sup>.

In order to distinguish between two scenarios of possible  $\text{Co}^{3+}$  spin state in the layered  $\text{Sr}_2\text{Co}_{0.5}\text{Ir}_{0.5}\text{O}_4$  at 7.6 GPa with the total spin state  $S=1$ , namely a mixture of HS- $\text{Co}^{3+}$  and LS- $\text{Co}^{3+}$  and pure IS- $\text{Co}^{3+}$ , we drew the difference spectra of Co- $K\beta$  emissions obtained between ambient pressure (AP) and 40 GPa (red line) as well as between 7.6 GPa and 40 GPa (blue line) shown in Fig. 3 (below the X-ray emission spectra). The red line corresponds to the change in the spin number  $\Delta S=2$ , while the blue line describes the change in the spin number  $\Delta S=1$ . These two difference spectra are almost identical apart from the scale factor of 2, used for the blue line, what is consequent with the scenario “1:1 mixture of HS- $\text{Co}^{3+}$  and LS- $\text{Co}^{3+}$  at 7.6 GPa”. Thus, the difference of the spectra does not show any sign for new features which would be expected for the presence of an intermediate spin state of  $\text{Co}^{3+}$ . Therefore, a continuous spin state transition from HS- $\text{Co}^{3+}$  to LS- $\text{Co}^{3+}$  under pressures in  $\text{Sr}_2\text{Co}_{0.5}\text{Ir}_{0.5}\text{O}_4$  can be verified. Note that in contrast to the nearly monotonous change of the IAD of  $\text{SrCo}_{0.5}\text{Ru}_{0.5}\text{O}_3$  with the pressure<sup>29</sup>, in the case of  $\text{Sr}_2\text{Co}_{0.5}\text{Ir}_{0.5}\text{O}_4$  the IAD decreases fast up to 10–12 GPa following by slower decreasing at higher pressures. It might be related to the anisotropy compression of  $\text{Sr}_2\text{Co}_{0.5}\text{Ir}_{0.5}\text{O}_4$  observed in the previous study<sup>28</sup>.

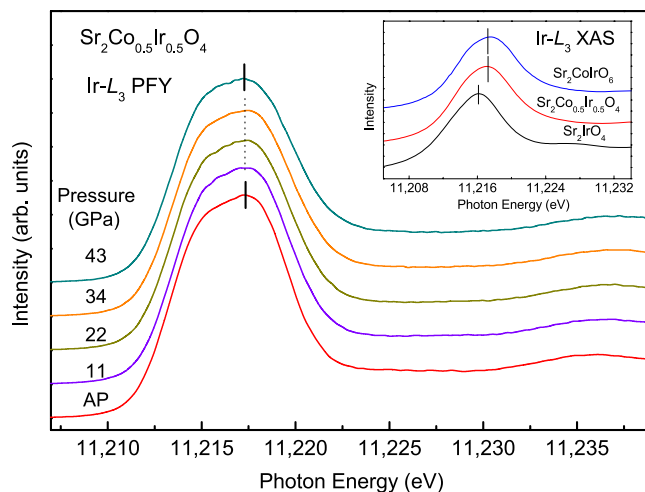


**Figure 5.** Pressure-dependence of the Ir- $L_3$  PFY spectra of  $\text{Sr}_2\text{Co}_{0.5}\text{Ir}_{0.5}\text{O}_4$ . Inset shows the Ir- $L_3$  XAS spectra of  $\text{Sr}_2\text{Co}_{0.5}\text{Ir}_{0.5}\text{O}_4$ ,  $\text{Sr}_2\text{IrO}_4$  as an  $\text{Ir}^{4+}$  reference and of  $\text{Sr}_2\text{CoIrO}_6$ <sup>42</sup> as an  $\text{Ir}^{5+}$  reference for comparison.

**Ir- $L_3$  X-ray absorption under pressure.** At this point we also would like to know whether the reduction of Co spin moment under pressure results from a change of the Co configuration from HS  $\text{Co}^{3+}$  ( $S=2$ ) to LS  $\text{Co}^{4+}$  ( $S=1/2$ ) accompanying with a change of the Ir valence state from  $5+$  to  $4+$ . For this purpose, we measured the partial fluorescence spectra at the Ir- $L_3$  edge of  $\text{Sr}_2\text{Co}_{0.5}\text{Ir}_{0.5}\text{O}_4$  under pressures up to 43 GPa. As shown in Fig. 5, from bottom to top, there is no energy shift of the Ir- $L_3$  PFY XAS spectra with the external pressures from AP to 43 GPa, indicating that the Ir valence remains  $5+$ , since a reduction of Ir valence state would lead to an energy shift to lower photon energies. As shown in inset of Fig. 5, the Ir- $L_3$  XAS spectrum of  $\text{Sr}_2\text{Co}_{0.5}\text{Ir}_{0.5}\text{O}_4$  measured in a transmission mode at ambient pressure is at higher photon energies compared with that of  $\text{Sr}_2\text{IrO}_4$  with  $\text{Ir}^{4+}$ , but locates at nearly the same photon energy as that of  $\text{Sr}_2\text{CoIrO}_6$  with  $\text{Ir}^{5+}$ <sup>42</sup>. Thus, we reaffirm that the decrease of the cobalt moment under pressure is solely due to a gradual spin state transition of  $\text{Co}^{3+}$  ions without any change in the valence state of the Co ions and also reaffirm the  $\text{Ir}^{5+}$  valence state, fulfilling the charge balance requirement for  $\text{Co}^{3+}/\text{Ir}^{5+}$  valence states in the studied  $\text{Sr}_2\text{Co}_{0.5}\text{Ir}_{0.5}\text{O}_4$  sample.

## Discussion

Using the element selective Co- $K$  EXAFS (extended X-ray absorption fine structure) we can determine Co-O distance at ambient pressure<sup>28</sup>. If we assumed that the pressure-induced variation of the Co-O bond lengths would be proportional to the variation of the lattice parameters, then we estimated Co-O bond lengths as a function of pressure from the lattice parameters obtained in the previous high pressure study<sup>28</sup>, as presented in Fig. 6(a). Please note that under external pressures, a  $\text{CoO}_6$  octahedron might rotate in the basal plane, as observed in the study on  $\text{Sr}_2\text{RuO}_4$  and  $\text{Sr}_2\text{IrO}_4$ <sup>27</sup>. Therefore, the reduction of the in-plane Co-O bond distances might be overestimated. However, our theoretical predication of the total energies of HS, LS and IS states as a function of in-plane and out-plane Co-O distances response to external pressure in general is still valid. One can see that the in-plane Co-O distance ( $\text{Co-O}_{\text{in-plane}}$  blue squares) reduces faster than that for the apex ( $\text{Co-O}_{\text{apex}}$  red circles) up to 10 GPa, namely  $\text{Co-O}_{\text{apex}}/\text{Co-O}_{\text{in-plane}}$  (black line) increases with high pressure<sup>26</sup>. One would expect that the IS ground state of  $\text{Co}^{3+}$  ion with one electron in  $e_g$  orbital could be stabilized under high pressure as the tetragonal distortion increases with high pressure. It is puzzled, however, our above Co  $K\beta$  X-ray emission spectra indicate a pressure-induced spin state transition from the HS state to the LS state without crossing the IS state.

To understand above experimental observation on the spin state transition, we have calculated the total energies of the LS, IS, and HS states as a function of pressure by taking the estimated  $\text{Co-O}_{\text{apex}}$  bond length and  $\text{Co-O}_{\text{in-plane}}$  bond length into account using the configuration-interaction cluster calculation. The hybridization part is obtained according to the Harrison's rules and the ionic crystal field is calculated as the Madelung potential. The factor of the Madelung potential can be determined because the HS and LS states are degenerated at 7.6 GPa, as observed in the Co  $K\beta$  X-ray emission spectra. The results are presented in Fig. 6(b). One can see in Fig. 6(b) that at ambient pressure, the ground state is the HS state consistent with the experimental  $\text{Co-L}_{2,3}$  XAS and Co  $K\beta$  X-ray emission results. Under external pressures up to 7.6 GPa, the LS and IS states gain more energies than the HS state due to the increase of  $10Dq$  because of a reduction of the Co-O bond lengths and to the enhancement of the  $e_g$  splitting ( $\Delta e_g$ ) from an increase of  $\text{Co-O}_{\text{apex}}/\text{Co-O}_{\text{in-plane}}$ , respectively. However, the energy gain of the LS  $\text{Co}^{3+}$  state ( $-24Dq$ ) overwhelms that of the IS  $\text{Co}^{3+}$  state ( $-14Dq-0.5\Delta e_g$ ). Therefore, as presented in Fig. 6(b), the LS state becomes the ground state when  $\text{Co-O}_{\text{apex}}/\text{Co-O}_{\text{in-plane}}$  is larger than 1.065 at the pressure about 7.6 GPa. When the external pressure is larger than 9.7 GPa, the LS state becomes even more stable against the HS and the IS owing to the further increase in  $10Dq$  and also a reduction of  $\Delta e_g$  as  $\text{Co-O}_{\text{apex}}/\text{Co-O}_{\text{in-plane}}$  decreases. As shown in Fig. 6(b), the IS state will never be the ground state under the pressure performed for the layered  $\text{Sr}_2\text{Co}_{0.5}\text{Ir}_{0.5}\text{O}_4$ , and thus one might wonder what is the condition to stabilize the IS state as a ground state for  $\text{Co}^{3+}$ .

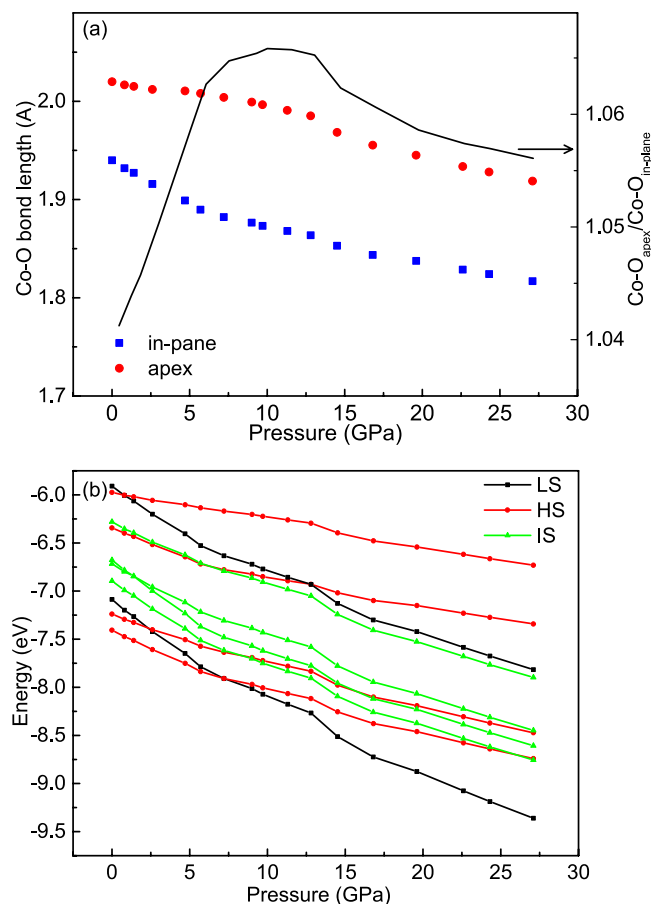


**Figure 6.** (a) Co-O<sub>apex</sub> bond length (red circles) and Co-O<sub>in-plane</sub> bond length (blue squares) as well as the ratio Co-O<sub>apex</sub>/Co-O<sub>in-plane</sub> (black line) as a function of the external pressure derived from ref. 28. Note that the reduction of the in-plane Co-O bond distance might be overestimated due to the possible rotation of the CoO<sub>6</sub> octahedron. (b) The energy diagram of three spin states as a function of the pressure using Co-O bond lengths in (a).

In order to scrutinize the stable conditions for the IS Co<sup>3+</sup> state in the layered structure, we have calculated the phase diagram of the ground state as a function of Co-O<sub>apex</sub> and Co-O<sub>in-plane</sub>. The phase diagram shown in Fig. 7 indicates that the strong elongated tetragonal distortion indeed could stabilize the IS state if the in-plane Co-O distance (Co-O<sub>in-plane</sub>) is rather short and ratio of Co-O<sub>apex</sub>/Co-O<sub>in-plane</sub> is quite large. In other words, the short in-plane Co-O bond length as well as the strong tetragonal distortion favors IS. However, if the Co-O<sub>in-plane</sub> is larger than 1.90 Å, the IS state will be hardly stabilized. Therefore, IS cannot be stabilized by heating the sample as illustrated with the blue line where the Co-O distance increases with temperature by keeping the ratio of Co-O<sub>apex</sub>/Co-O<sub>in-plane</sub> at room temperature in Fig. 7. On the other hand, the presence of the IS ground state might be possible in TlSr<sub>2</sub>CoO<sub>5</sub>, where one of two Co<sup>3+</sup> sites at low temperatures (O-phase) has a small value of the Co-O<sub>in-plane</sub> = 1.79 Å and Co-O<sub>apex</sub> = 2.19 Å, presented as a green circle in Fig. 7<sup>43,44</sup>. Besides, the Co-O bond lengths (magenta circles) in Sr<sub>2</sub>Co<sub>0.5</sub>Ir<sub>0.5</sub>O<sub>4</sub> under external pressures are plotted in this phase diagram. One can see that the ground state of Co<sup>3+</sup> ion in Sr<sub>2</sub>Co<sub>0.5</sub>Ir<sub>0.5</sub>O<sub>4</sub> has a stable HS state and is transformed to the LS state with the external pressures without crossing the IS state (magenta circles). On the other hand, the Co-O bond distance of LaCoO<sub>3</sub> is reduced from 1.9329 Å to 1.888 Å crossing a mixed HS/LS state to a pure LS state with pressure<sup>39</sup>. The mixed spin state of LaCoO<sub>3</sub> is due to the much shorter Co-O bond distance, close to the boundary of the HS and LS, as compared with that of Sr<sub>2</sub>Co<sub>0.5</sub>Ir<sub>0.5</sub>O<sub>4</sub> (Co-O<sub>in-plane</sub> = 1.967 Å and Co-O<sub>apex</sub> = 2.020 Å)<sup>28</sup>.

## Conclusion

We have studied the valence state and spin state transition of Co ion under external pressures in a hybrid 3d-5d transition metals solid-state oxide Sr<sub>2</sub>Co<sub>0.5</sub>Ir<sub>0.5</sub>O<sub>4</sub> using hard X-ray absorption and Co-Kβ emission spectroscopies. The high spin state of Co<sup>3+</sup> ions found at ambient pressure exhibits a complete spin state transition to the low-spin state up to 40 GPa without crossing the intermediate-spin state, while the valence state of Ir<sup>5+</sup> ions remains unchanged. At external pressures below 9.7 GPa, the fast increase of the ratio of Co-O<sub>apex</sub>/Co-O<sub>in-plane</sub> does not stabilize the IS state but the LS state instead owing to a rapid increase of 10Dq overwhelming the Jahn-Teller distortion of the e<sub>g</sub> orbitals. Above 9.7 GPa, the LS state becomes even more stable due to the decrease of the ratio of Co-O<sub>apex</sub>/Co-O<sub>in-plane</sub>. To determine the condition for stabilizing a possible intermediate-spin ground state in such a layered oxide, we have compared the energies of the three different spin states of Co<sup>3+</sup> ions



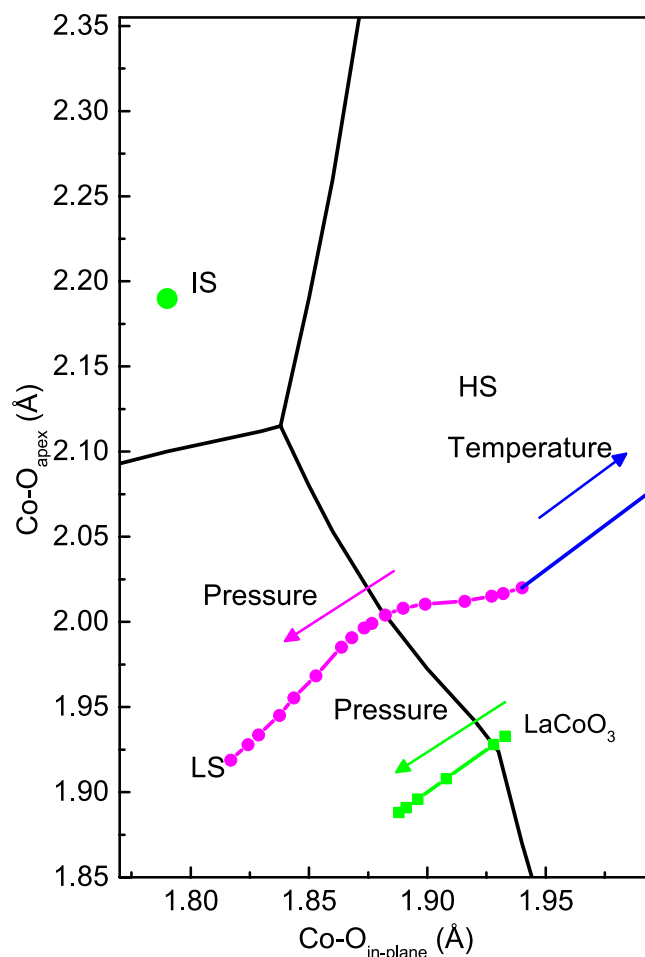


**Figure 7.** The phase diagram of the ground state of  $\text{Co}^{3+}$  as a function of Co-O bond lengths. The magenta circles are the Co-O bond lengths of  $\text{Sr}_2\text{Co}_{0.5}\text{Ir}_{0.5}\text{O}_4$  estimated from ref. 28 and the blue line refers to an increase of its Co-O distance with temperature by keeping the ratio of  $\text{Co-O}_{\text{apex}}/\text{Co-O}_{\text{in-plane}}$  at room temperature. The green circle is those of one of two  $\text{Co}^{3+}$  sites in the O-phase in  $\text{TlSr}_2\text{CoO}_5$ <sup>43</sup>. The green line represents the Co-O distances of  $\text{LaCoO}_3$ <sup>39</sup> with pressure.

as a function of bond lengths. These results have been plotted in a phase diagram and a stable IS state can only be found when the in-plane Co bond length is substantially shorter than the  $\text{Co-O}_{\text{apex}}$  bond length.

## Methods

**Sample synthesis.** The layered polycrystalline  $\text{Sr}_2\text{Co}_{0.5}\text{Ir}_{0.5}\text{O}_4$  was synthesized from solid state reaction as described previously<sup>28</sup>. The purity and unit cell parameters were determined by X-ray powder diffraction (XPD).  $\text{Sr}_2\text{Co}_{0.5}\text{Ir}_{0.5}\text{O}_4$  is more insulating than  $\text{Sr}_2\text{IrO}_4$ <sup>45</sup>, as indicated by the resistivity data in Fig. S1 in the Supplementary Information.

**X-Ray spectroscopy.** The  $\text{Co-L}_{2,3}$  X-ray absorption spectroscopy (XAS) measurements were recorded at the BL11A beam line of the National Synchrotron Radiation Research Center (NSRRC) in Taiwan. Clean sample surfaces were obtained by cleaving pelletized samples *in situ* in an ultra-high vacuum chamber with a pressure of  $10^{-10}$  mbar range. The  $\text{Co-L}_{2,3}$  spectra were collected at room temperature using total electron yield mode (TEY) with an energy resolution of about 0.3 eV. The high-pressure Co-K and Ir-L<sub>3</sub> partial-fluorescence-yield (PFY) XAS spectra and Co  $K\beta$  X-ray emission spectra were obtained at the Taiwan inelastic X-ray scattering BL12XU beamline at SPring-8 in Japan. A Mao-Bell diamond anvil cell with a Be gasket was used for the high-pressure experiment. Silicone oil served as a medium to transmit pressure. The applied pressure in the diamond anvil cell was measured through the Raman line shift of ruby luminescence before and after each spectral collection. The Co  $K\beta$  X-ray emission spectra were collected at  $90^\circ$  from the incident X-ray and analyzed with a spectrometer (Johann type) equipped with a spherically bent Ge(444) crystal and Si(553) (radius 1 m), respectively, arranged on a horizontal plane in a Rowland-circle geometry.

## References

1. Imada, M., Fujimori, A. & Tokura, Y. Metal-insulator transitions. *Rev. Mod. Phys.* **70**, 1039–1263 (1998).
2. Kim, B. J. *et al.* Novel Jeff=1/2 Mott State Induced by Relativistic Spin-Orbit Coupling in  $\text{Sr}_2\text{IrO}_4$ . *Phys. Rev. Lett.* **101**, 076402 (2008).

3. Kim, B. J. *et al.* Phase-Sensitive Observation of a Spin-Orbital Mott State in  $\text{Sr}_2\text{IrO}_4$ . *Science* **323**, 1329–1332 (2009).
4. Matsuno, J. *et al.* Metallic Ferromagnet with Square-Lattice  $\text{CoO}_2$  Sheets. *Phys. Rev. Lett.* **93**, 167202 (2004).
5. Wang, X. L. & Takayama-Muromachi, E. Magnetic and transport properties of the layered perovskite system  $\text{Sr}_{2-y}\text{Y}_y\text{CoO}_4$  ( $0 \leq y \leq 1$ ). *Phys. Rev. B* **72**, 064401 (2005).
6. Matsuno, J. *et al.* Novel metallic ferromagnet  $\text{Sr}_2\text{CoO}_4$ . *Thin Solid Films* **486**, 113–116 (2005).
7. Matsuno, J., Okimoto, Y., Kawasaki, M. & Tokura, Y. Variation of the Electronic Structure in Systematically Synthesized  $\text{Sr}_2\text{MO}_4$  ( $M = \text{Ti, V, Cr, Mn, and Co}$ ). *Phys. Rev. Lett.* **95**, 176404 (2005).
8. Lee, K.-W. & Pickett, W. E. Correlation effects in the high formal oxidation-state compound  $\text{Sr}_2\text{CoO}_4$ . *Phys. Rev. B* **73**, 174428 (2006).
9. Pandey, S. K. Correlation induced half-metallicity in a ferromagnetic single-layered compound:  $\text{Sr}_2\text{CoO}_4$ . *Phys. Rev. B* **81**, 035114 (2010).
10. Wu, H. Metal-insulator transition in  $\text{Sr}_{2-y}\text{La}_y\text{CoO}_4$  driven by spin-state transition. *Phys. Rev. B* **86**, 075120 (2012).
11. Shimada, Y., Miyasaka, S., Kumai, R. & Tokura, Y. Semiconducting ferromagnetic states in  $\text{La}_{1-x}\text{Sr}_{1+x}\text{CoO}_4$ . *Phys. Rev. B* **73**, 134424 (2006).
12. Chichev, A. V. *et al.* Structural, magnetic, and transport properties of the single-layered perovskites  $\text{La}_{2-x}\text{Sr}_x\text{CoO}_4$  ( $x = 1.0-1.4$ ). *Phys. Rev. B* **74**, 134414 (2006).
13. Wu, H. High-spin and low-spin mixed state in  $\text{LaSrCoO}_4$ : An *ab initio* study. *Phys. Rev. B* **81**, 115127 (2010).
14. Hollmann, N. *et al.* Evidence for a temperature-induced spin-state transition of  $\text{Co}^{3+}$  in  $\text{La}_{2-x}\text{Sr}_x\text{CoO}_4$ . *Phys. Rev. B* **83**, 174435 (2011).
15. Merz, M. *et al.* Spin and orbital states in single-layered  $\text{La}_{2-y}\text{Ca}_y\text{CoO}_4$  studied by doping- and temperature-dependent near-edge x-ray absorption fine structure. *Phys. Rev. B* **84**, 014436 (2011).
16. Moritomo, Y., Higashi, K., Matsuda, K. & Nakamura, A. Spin-state transition in layered perovskite cobalt oxides:  $\text{La}_{2-y}\text{Sr}_y\text{CoO}_4$  ( $0.4 \leq x \leq 1.0$ ). *Phys. Rev. B* **55**, R14725–R14728 (1997).
17. Tsujimoto, Y. *et al.* Crystal Structural, Magnetic, and Transport Properties of Layered Cobalt Oxyfluorides,  $\text{Sr}_2\text{CoO}_{3+x}\text{F}_{1-x}$  ( $0 \leq x \leq 0.15$ ). *Inorg. Chem.* **51**, 4802–4809 (2012).
18. Ou, X., Fan, F., Li, Z., Wang, H. & Wu, H. Spin-state transition induced half metallicity in a cobaltate from first principles. *Appl. Phys. Lett.* **108**, 092402 (2016).
19. Tsujimoto, Y. *et al.* Crystal Pressure-Driven Spin Crossover Involving Polyhedral Transformation in Layered Perovskite Cobalt Oxyfluoride. *Sci. Rep.* **6**, Article number: 36253 (2016).
20. Gatimu, A. J., Berthelot, R., Muir, S., Sleight, A. W. & Subramanian, M. A. Synthesis and characterization of  $\text{Sr}_2\text{Ir}_{1-x}\text{M}_x\text{O}_4$  ( $M = \text{Ti, Fe, Co}$ ) solid solutions. *J. Solid State Chem.* **190**, 257–263 (2012).
21. Calder, S. *et al.* Magnetic structural change of  $\text{Sr}_2\text{IrO}_4$  upon Mn doping. *Phys. Rev. B* **86**, 220403 (2012).
22. Ou, X. & Wu, H. Coupled charge-spin-orbital state in Fe- or Co-doped  $\text{Sr}_2\text{IrO}_4$ . *Phys. Rev. B* **89**, 035138 (2014).
23. Hollmann, N. *et al.* Electronic and magnetic properties of the kagome systems  $\text{YBaCo}_4\text{O}_7$  and  $\text{YBaCo}_3\text{MO}_7$  ( $M = \text{Al, Fe}$ ). *Phys. Rev. B* **80**, 085111 (2009).
24. Hu, Z. *et al.* Different Look at the Spin State of  $\text{Co}^{3+}$  Ions in a  $\text{CoO}_2$  Pyramidal Coordination. *Phys. Rev. Lett.* **92**, 207402 (2004).
25. Haverkort, M. W. *et al.* Spin State Transition in  $\text{LaCoO}_3$  Studied Using Soft X-ray Absorption Spectroscopy and Magnetic Circular Dichroism. *Phys. Rev. Lett.* **97**, 176405 (2006).
26. Hu, Z. *et al.* Spin-state order/disorder and metal-insulator transition in  $\text{GdBaCo}_2\text{O}_{5.5}$ : experimental determination of the underlying electronic structure. *New J. Phys.* **14**, 123025 (2012).
27. Huang, Q. *et al.* Neutron Powder Diffraction Study of the Crystal Structures of  $\text{Sr}_2\text{RuO}_4$  and  $\text{Sr}_2\text{IrO}_4$  at Room Temperature and at 10 K. *J. Solid State Chem.* **112**, 355 (1994).
28. Mikhailova, D. *et al.* Charge Transfer and Structural Anomaly in Stoichiometric Layered Perovskite  $\text{Sr}_2\text{Co}_{0.5}\text{Ir}_{0.5}\text{O}_4$ . *Eur. J. Inorg. Chem.* **2017**, 587–595 (2017).
29. Chen, J.-M. *et al.* A Complete High-to-Low spin state Transition of Trivalent Cobalt Ion in Octahedral Symmetry in  $\text{SrCo}_{0.5}\text{Ru}_{0.5}\text{O}_{3.6}$ . *J. Am. Chem. Soc.* **136**(4), 1514–1519 (2014).
30. Groot, F. M. F. de X-ray absorption and dichroism of transition metals and their compounds. *J. Electron Spectrosc. Relat. Phenom.* **67**, 529–622 (1994).
31. Tanaka, A. & Jo, T. Resonant  $3d$ ,  $3p$  and  $3s$  Photoemission in Transition Metal Oxides Predicted at  $2p$  Threshold. *J. Phys. Soc. Jpn.* **63**, 2788–2807 (1994).
32. Udd = 5.5 eV, Upd = 7.0 eV;  $\Delta = 2.0$  eV; The Slater integrals were reduced to 80% of their Hartree-Fock values.
33. Herrero-Martín, J. *et al.* Spin-state transition in  $\text{Pr}_{0.5}\text{Ca}_{0.5}\text{CoO}_3$  analyzed by x-ray absorption and emission spectroscopies. *Phys. Rev. B* **86**, 125106 (2012).
34. Vankó, G., Rueff, J.-P., Mattila, A., Németh, Z. & Shukla, A. Temperature- and pressure-induced spin-state transitions in  $\text{LaCoO}_3$ . *Phys. Rev. B* **73**, 024424 (2006).
35. Chen, J. M. *et al.* Evolution of spin and valence states of  $(\text{Pr}_{0.7}\text{Sm}_{0.3})_{0.7}\text{Ca}_{0.3}\text{CoO}_3$  at high temperature and high pressure. *Phys. Rev. B* **90**, 035107 (2014).
36. Tsutsumi, K., Nakamori, H. & Ichikawa, K. X-ray Mn  $K\beta$  emission spectra of manganese oxides and manganates. *Phys. Rev. B* **13**, 929–933 (1976).
37. Oka, K. *et al.* Pressure-Induced Spin-State Transition in  $\text{BiCoO}_3$ . *J. Am. Chem. Soc.* **132**(27), 9438–9443 (2010).
38. Kozlenko, D. P. *et al.* Temperature- and pressure-driven spin-state transitions in  $\text{LaCoO}_3$ . *Phys. Rev. B* **75**, 064422 (2007).
39. Vogt, T., Hriljac, J. A., Hyatt, N. C. & Woodward, P. Pressure-induced intermediate-to-low spin state transition in  $\text{LaCoO}_3$ . *Phys. Rev. B* **67**, 140401 (2003).
40. Baier, J. *et al.* Spin-state transition and metal-insulator transition in  $\text{La}_{1-x}\text{Eu}_x\text{CoO}_3$ . *Phys. Rev. B* **71**, 014443 (2005).
41. Cwik, M. The Interplay of Lattice, Spin, and Charge Degrees of Freedom in Layered Cobaltates. Ph.D. Dissertation, Universität of Cologne, Cologne, 2007.
42. Mikhailova, D. *et al.* Oxygen-driven competition between low-dimensional structures of  $\text{Sr}_3\text{CoMO}_6$  and  $\text{Sr}_3\text{CoMO}_{7-8}$  with  $M = \text{Ru, Ir}$ . *Dalton Trans.* **43**, 13883–13891 (2014).
43. Doumerc, J.-P. *et al.* Crystal structure of the thallium strontium cobaltite  $\text{TlSr}_2\text{CoO}_5$  and its relationship to the electronic properties. *J. Mater. Chem.* **11**, 78–85 (2001).
44. Doumerc, J.-P., Grenier, J.-C., Hagenmuller, P., Pouchard, M. & Villesuzanne, A. Interplay between Local Electronic Configuration and the Occurrence of a Metallic State: An Experimental Approach. *J. Solid State Chem.* **147**, 211–217 (1999).
45. Kini, N. S., Strydom, A. M., Jeevan, H. S., Geibel, C. & Ramakrishnan, S. Transport and thermal properties of weakly ferromagnetic  $\text{Sr}_2\text{IrO}_4$ . *J. Phys.: Condens. Matter* **18**, 8205–8216 (2006).

## Acknowledgements

This work is supported by the Ministry of Science and Technology under Grant Nos. MOST 102-2112-M-213 -004 -MY3 and MOST 105-2113-M-213 -005 -MY3 and in Dresden supported by the Deutsche Forschungsgemeinschaft through SFB 1143.



### Author Contributions

D.M. prepared the sample in this study. Z.H., C.Y.K., J.M.L., S.C.H., S.A.C., W.S., H.I., N.H., Y.F.L., K.D.T., C.T.C., L.H.T., and J.M.C. conducted the experiments. Y.Y.C., H.J.L., Z.H., and A.T. conducted the cluster calculations. Y.Y.C., H.J.L., Z.H., J.M.C., and L.H.T. wrote the paper. All authors reviewed the manuscript.

### Additional Information

**Supplementary information** accompanies this paper at doi:[10.1038/s41598-017-03950-z](https://doi.org/10.1038/s41598-017-03950-z)

**Competing Interests:** The authors declare that they have no competing interests.

**Publisher's note:** Springer Nature remains neutral with regard to jurisdictional claims in published maps and institutional affiliations.



**Open Access** This article is licensed under a Creative Commons Attribution 4.0 International License, which permits use, sharing, adaptation, distribution and reproduction in any medium or format, as long as you give appropriate credit to the original author(s) and the source, provide a link to the Creative Commons license, and indicate if changes were made. The images or other third party material in this article are included in the article's Creative Commons license, unless indicated otherwise in a credit line to the material. If material is not included in the article's Creative Commons license and your intended use is not permitted by statutory regulation or exceeds the permitted use, you will need to obtain permission directly from the copyright holder. To view a copy of this license, visit <http://creativecommons.org/licenses/by/4.0/>.

© The Author(s) 2017